BRAIN TUMOR CLASSIFICATION AND SEGMENTATION BY USING RESENT MACHINE LEARNING CLASSIFIER

Arif kamal[1], Emad Ud Din Zafar[2], Muhammad Ibtisam Abid[3], Ijaz Ahmad[1], Waseem Hussain[1],

1. Department of Computer science, Islamia collage Peshawar Khyber Pakhtunkhwa Pakistan.
2. Department of Computer science, CECOS University of IT and Emerging Sciences Peshawar, Khyber Pakhtunkhwa Pakistan.
3. Department of Computer networks and security, FAST National University of Computer and Emerging Sciences, Islamabad Campus.

ABSTRACT:

The brain tumor is situated in the brain of patient they might extremely threaten their life. The influence and outcome of the factor of brain tumor to improve treatment and controlled the disease. For identification of brain tumors, various studies have been carried out. In addition, laborious with respect to execution time and laboratory equipment some of them were expensive though others have not expressed the desired results. A research study we are used segmentation and classification through intelligent computational model for brain tumor. This schema of study using 2013 BRATS dataset four modalities of MRI. The required range and pre-processing image applied the different techniques for the achievement of numerical attributes for segment area like enhancing tumor, complete tumor and core tumor. The total number of 58 feature are removed. Now the random forest (RF) use for the training and testing for feature array. The proposed model used the 10 cross validation method to enhance the performance of model. The proposed model shows the better results as compare to the other machine learning.
Keywords: Brain tumor segmentation, feature extraction, Resent classifier.

Introduction

In this paper, we aim to improve a brain tumor segmentation and diagnosis automated system in a precise, reliable, and effective manner. Our study focuses on enhancing tumor visualization by cascading segmenting various regions. The entire portion of the brain affected by the tumor is separated from the healthy brain in the initial stage, i.e. E. Completely grown out tumor [1]. The second stage involves separating the primary and central tumor from the already segmented tumorous brain. This region of the tumor-filled brain is referred to as the "Tumor Core." In the last phase, segmentation is our main concern. A portion of a tumor that is actively spreading inside of a healthy brain is referred to as an "enhancing tumor." A portion of a tumor that is actively spreading inside of a healthy brain is called an enhancing tumor [2]. Radiotherapy, including head X-rays and CT scans, genetic conditions, skull fractures, and diseases like HIV and AIDS, among other things, can cause brain tumors to form in patients. The brain can suffer serious damage if abnormal cells grow into a mass in the rigidly constrained space. Primary and secondary brain tumors are the two different varieties. Brain-based primary tumors are the most common type of cancer. Secondary brain tumors are a subtype of tumor in which cancerous cells spread to new body parts, typically with the help of the bloodstream, and are triggered by various cancer types, such as lung cancer, breast cancer, or liver cancer [3]. The majority of brain tumor deaths occur in males and females younger than 20. However, brain tumor deaths also occur most frequently in males and females between the ages of 20 and 39. The American Cancer Society puts together a report each year that details the expected incidence rates of various cancers in both men and women as well as the total number of fatalities anticipated in the USA only [4]. The US society predicted that in 2015 there would be 22,850 new cases of cancer involving the nervous system, including the brain. The likelihood of patients in the 22,850 new cases is that nearly 12,850 of them will be men, and 10,000 will be women. In 2015, 15,320 deaths are predicted, with 6,370 deaths expected for women and 8,950 deaths for men [5].

1. Material and Methods.

1.1 Dataset

This dataset contains different number of images of human brain MRI images, which are classified into four classes: this is the name of the folders containing the images of training data.

1. Glioma_tumor
2. meningioma tumor
3. no_tumor
4. pituitary_tumor

There are 2870 images, which is used for training model, and 394 images are used for testing the performance of the proposed system.

1. Glioma_tumor
2. meningioma_tumor
3. no_tumor
4. pituitary_tumor

Similarly, this label also contains the list of folder containing the data for testing the proposed model. The loaded images are normalized by dividing each pixel value by 255 to bring it into the range of 0 to 1. Finally, the shape of the **x_train** and **x_test** arrays are printed to verify that the images are loaded correctly.

1.2 Categorization Schemes for Brain tumor segmentation

Due to their complexity, brain tumor classification and sub-division into different types has become a difficult research area in recent years. Neurologists and other medical professionals find it difficult to distinguish between a cancerous brain and a healthy brain from available brain scan images when using different neuroimaging techniques [06]. The tumor segmentation is broken down into the following main categories: (i) Manual assessment; (ii) Semi-automated separation; and (iii) Automated segmentation [07-08]. Neurologists and other medical professionals diagnose brain tumors during manual segmentation assessment, analyze their grades, and mark the tumors using various software programs. To accurately diagnose a tumor, manual segmentation is a time-consuming task that demands significant effort. Semi-automated segmentation helps to shorten this labor-intensive task. This method greatly reduces the need for human involvement, but it still necessitates experts to oversee the software. The presentation of several partially automated systems has taken place [09-10-11-12]. Fully automated segmentation further enhances semi-automated segmentation because human involvement in the classification and dissection of brain tumors is eliminated. It has been widely used to segment brain tumors using fully automated segmentation [23, 21, 1, 3, 11, 5, 9, 19, 25, 27]. The majority of researchers classified brain tumors using either machine learning or image acquisition and processing techniques. In our research, we have concentrated on using both machine learning (ML) and image processing techniques for segmentation and classification. Machine learning classification can be divided into two main categories: supervised learning and unsupervised learning [26]. In unsupervised learning, images are segmented when the pixels or voxels of the image are unlabeled, such as in cluster analysis, in which various pixels or voxels of the image are combined into different clusters based on their features. Each cluster (Cluster) of pixels or voxels stands for a particular category. The labels of the voxels, on the other hand, are predetermined in supervised learning. We used a supervised learning algorithm to categorize the pixels or voxels because the ground truth for each patient in the BRATS 2013 dataset is fully known. In the Categorization scheme [12, 29, 28], which is described in the following paragraph, for classifying and segmenting brain tumors, pixel classification is a sub-category. The majority of the algorithms, systems, and various techniques put forth by various researchers for the classification and segmentation of brain tumors can be divided into the following groups: (a) threshold-based, (b) region-based, (c) prototypical-based, and (d) voxel classification techniques [12, 29, 28]. Different classes are given to voxels by threshold-based techniques. By comparing each voxel of the image with a predetermined threshold, these classes are determined. The two categories of global thresholding and local thresholding are further separated into [12, 29, and 28]. The algorithms that make up the area-based segmentation technique define a specific similarity criterion in advance, and after that, different disjoint regions are constructed by absorbing nearby pixels with similar characteristics. A further division of region-based algorithms is made into (a) techniques for a region's budding and (b) techniques for a region's watershed [12, 29, and 28]. Model technique serves as the foundation for the third type of classification/segmentation method. A number of the image's (object's) properties, e. G. Position, shape, orientation, etc. A connected and continuous model for a specific anatomic structure was built using.

Parametric deformable models and geometric deformable models are the other groups into which these techniques are further divided [12, 29, and 28]. Each pixel's context, intensity, and neighborhood features vary across the images as a whole, which is characterized by a feature space. For classifying the pixels (voxels), supervised and unsupervised algorithms can be used. Based on the voxel's feature set in the feature space. As was already mentioned, the sole basis of our work is a supervised learning algorithm that, after being trained in the training phase, allows for the classification of pixels or voxels in the testing phase. For this purpose, many ML algorithms are employed. Support Vector Machines (SVM), Bayesian classifiers, Random Decision Forest (RDF), and Artificial Neural Networks (ANN) are a few of the more well-known algorithms. For the classification of brain tumors in our study, we employ the resent.

2. Proposed Scheme

All MRI sequences, including T1-w, T2-w, T1-c, and Flair, have a pre-processing step that is the most important. With the aid of the histogram matching technique, the voxel intensities of the sequences are normalized during the pre-processing stage. This matching created an attractive image. To choose the best unit that can provide accurate histogram matching of cancerous classes, the MRI sequences (T1-w, T2-w, T1-c, and Flair) are first examined for all data sets. These allocations are made as a standard because they will also be used for testing and histogram matching in the future as show in the figure 3.1.

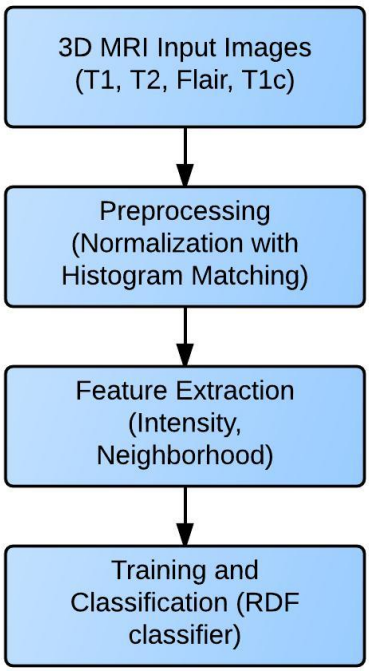

Figure 1.1 proposed scheme

2.1 Feature Extraction

After the pre-processing step, now the images are in standard format. Different intensity and neighborhood features are extracted in order to form a feature space. This thesis was initially intended to improve the results of base paper [9], in terms of both accuracy (Dice and Jaccard) and efficiency (time taken for a single test case).

2.2 Features used in base paper

The 316 features were used in the base paper. For the selection of areas and categorization of cancerous brain, RDF is also used. Below is a description of the specific characteristics of base paper. Intensities of MR sequences. Information about the local area.

- Contextual data.
- Texture.
- MR scans are intensities.

- Voxel intensity values and the absolute difference between six different combinations, i. E. In the feature vector, the independent features |T1 - T2|, |T1-T1c|, |T1-Flair|, |T2-T1c|, |T2-Flair|, and |T1c-Flair| are used.

Neighborhood information

The neighborhood feature vector contains the specific data. Now the characteristics are sum, mean, median of various windows. i.e 9x9x9, 15x15x15, 3x3x3, 19x19x19, and 3x3x3. Now the total feature are 40 with the ratio of (4 windows x 10 intensity values) of different 3D windows.

The total number of median, sum, and range features are 40 each in a similar manner. The total of all these neighborhood information features comes to 160 (16 mean 16 median 16 sum 16 range) features.

3. RESULTS AND DISCUSSION

In order to perform the classification on MRI images as normal or abnormal image in python, the following procedure can be used. This is first cell of the code and it shows the list of all prerequisites libraries, which are essential for the code implementation of the machine learning for images classification, and features extraction from MRI images. For instance, list of libraries with their version are as below.

python	3.7.12
tensor flow	2.6.0
keras	2.6.0
keras-preprocessing	1.1.2
Matplotlib	3.0.2
opencv	4.1.2
scikit-learn	0.22.2

Table 4.1

This dataset contains different number of images of human brain MRI images, which are classified into four classes: this is the name of the folders containing the images of training data.

1. Glioma_tumor
2. meningioma_tumor
3. no_tumor
4. pituitary_tumor

There are 2870 images, which is used for training model, and 394 images are used for testing the performance of the proposed system.

1. Glioma_tumor
2. meningioma_tumor
3. no_tumor
4. pituitary_tumor

Similarly, this label also contains the list of folder containing the data for testing the proposed model.

1. Creating labels for both class and each set of images.
2. Apply preprocess techniques (bilateral filtering and applying pseudo color map) on each images
3. As these images have different dimensions, the code resize it to its size of 200 X 200/
4. Storing them in the **x_train** and **x_test** lists. The corresponding labels for each image are also being stored in **y_train** and **y_test**.

The loaded images are normalized by dividing each pixel value by 255 to bring it into the range of 0 to 1.
Finally, the shape of the **x_train** and **x_test** arrays are printed to verify that the images are loaded correctly.

```
100%|██████████| 826/826 [00:57<00:00, 14.36it/s]
100%|██████████| 100/100 [00:05<00:00, 16.70it/s]
100%|██████████| 822/822 [00:18<00:00, 43.51it/s]
100%|██████████| 115/115 [00:07<00:00, 14.63it/s]
100%|██████████| 395/395 [00:05<00:00, 78.74it/s]
100%|██████████| 105/105 [00:06<00:00, 15.22it/s]
100%|██████████| 827/827 [00:12<00:00, 66.50it/s]
100%|██████████| 74/74 [00:04<00:00, 16.46it/s]

(2870, 200, 200, 3)
(394, 200, 200, 3)
```

Figure 1

This is the output of the above code snippet. The output show that there are 2870 images of dimension 200 X 200 and has only three-color channels. Similarly, the second line show that testing line also have 394 images which are resize to 200X200 and it has only three color channels.The **tight layout** is a python function, which is used to improve the spacing between the subplots. This code is used in order to find that whether images are preprocessed correctly or not. After running the code on our given dataset, it generate output as shown in figure below.

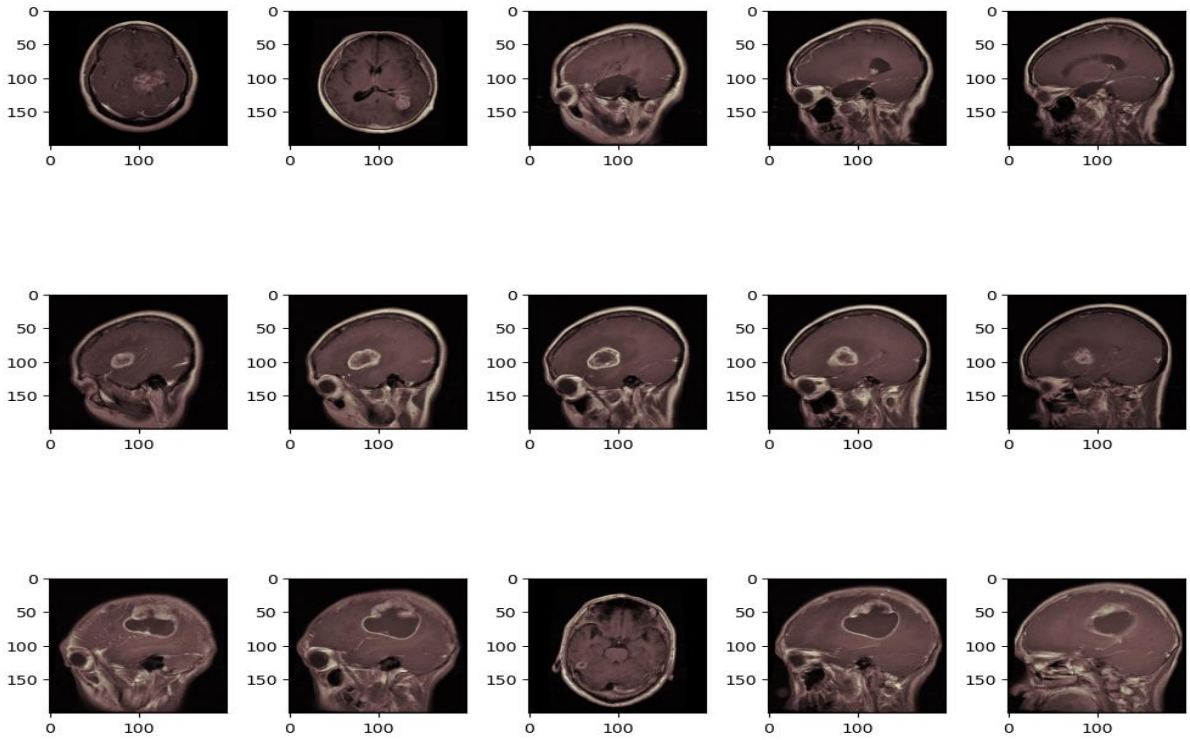

Figure 2

It can be analyzed from above figure that, each images have the same dimensions. This is a preprocessing task and which preprocessed all the data to overcome the issue of overfitting or under fitting problems. The Image data generator is configured with several parameters, such as rotation range, width_shift_range, height_shift_range, and horizontal flip, which specify the range of values for different types of random transformations that can be applied to the images. The datagen.fit (x_train) statement then fits the ImageDataGenerator object to the training data x_train. This step calculates the statistics required for the data augmentation such as mean, variance, etc., and prepares the Image data generator object for use during training. When the data augmentation is ready, now the model are created

4.1 Feature information

ResNet50 extracts a set of high-level features from an image. The features extracted include edges, corners, textures, and more complex pattern information. These features are extracted using convolutional layers, which learn to detect specific patterns in the image. The ResNet50 model has multiple layers, and each layer extracts more abstract and high-level features than the previous one. Final layer, the extracted features are input into a

fully connected layer that outputs the predicted class of the image.BATCH_SIZE = 64: This sets the batch size to 64, which is the number of samples, which update the model once. EPOCHS = 50: This sets the number of training epochs to 50. If the model does not work properly, then Early Stopping stops training if the validation loss does not improve by at least 0.001 for five consecutive epochs. From the results, it can analyzed that the classification accuracy of the proposed model increase with number of epoch, mean that after 1 epoch, the proposed model give the accuracy of 82.2 and after the 14 epoch, as the Early Stopping function stop the training as there is no improvement in learning rate. Proposed model achieve high accuracy as 99.14.

Accuracy graph.

The plot of training and validation loss as well as training, validation accuracy curves of the model, and the second plot shows the trend of training accuracy and validation accuracy over the epochs. After 14 epoch, after the 14 epoch, as the **Early Stopping** function stop the training, as there is no improvement in learning rate. The system stops training if the validation loss does not improve by at least 0.001 for five consecutive epochs.

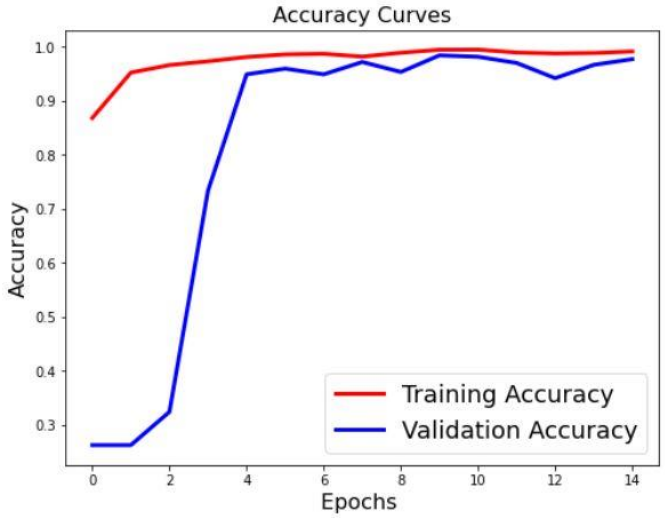

The above figure shows the accuracy of the model during the training phase. This curve can be used to find out how well the model is performing on the training data. As shown in the figure, the accuracy increases as the model learns and improves its ability to classify the images correctly. From the figure above, it can be analyzed that the model have no issues such as overfitting or under fitting during the training and testing phase.

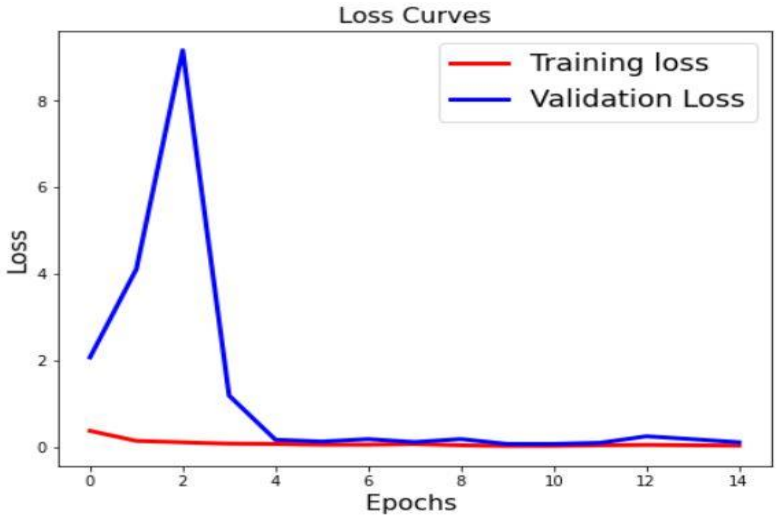

Figure above shows the trend of the average loss per batch or epoch during the training process over the epochs. It show the measure of the difference between the predicted outputs of the model and the true labels, and is

used to optimize the model's weights and biases during the backpropagation step of the training process. From the figure above, I can be analyzed that the average loss decrease with increasing the epoch numbers.

1. Glioma_tumor
2. meningioma_tumor
3. no_tumor
4. pituitary_tumor

	Precision	Recall	F1-score	Support
Glioma_tumor	.98	.99	.98	294
meningioma_tumor	.98	.97	.98	303
no_tumor	1.00	1.00	1.00	403
pituitary_tumor	.99	.99	.99	294
Classification Performance.				
Accuracy			.99	1294
Macro avg	.99	.99	.99	1294
Weight avg	.99	.99	.99	1294

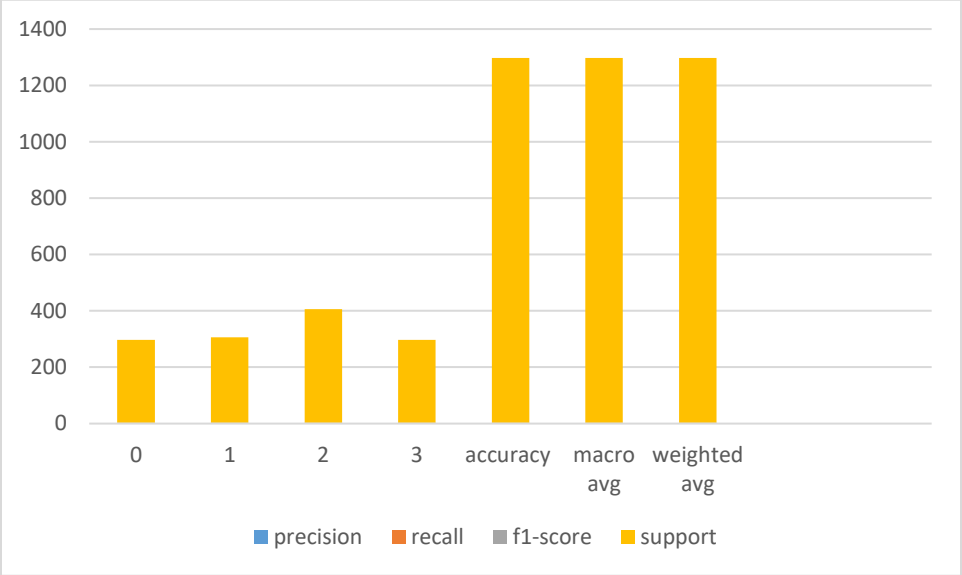

This output shows the classification report of a model's performance on a test set. The classification report provides evaluation metrics such as precision, recall, f1-score, and support for each class in the dataset. In this case, the model achieved an overall accuracy of 0.99 on the test set, meaning it correctly classified 99% of the images. For each class, the report shows precision, recall, and f1-score.**Precision** is the number of true positives (correctly classified images) divided by the total number of predicted positives (all images classified as belonging to that class),While **recall** is the number of true positives divided by the total number of actual positives (all images in that class). F1-score is the harmonic mean of precision and recall. The **macro avg** and **weighted avg** metrics provide an overall evaluation of the model's performance across all classes. The macro avg is the unweighted average of precision, recall, and f1-score across all classes, while the weighted avg is the weighted average of these metrics, weighted by the number of samples in each class.

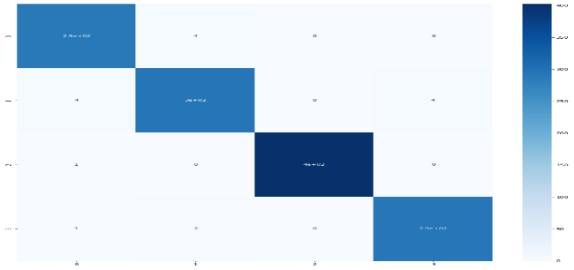

Figure 3

The above confusion matrix shows the performance of the proposed system.

From the confusion matrix figure, it can be shown that the 290 instances are correctly classified for **Glioma_tumor** class while only 4 images are classified incorrectly. For **meningioma tumor,** 300 instances are correctly classified as meningioma tumor instances, while only eight entries are classified as abnormal class. For **no_tumor** class, 400 images are classified correctly while only 1 image is misclassified. Similarly, **pituitary tumor,** 290 images are correctly classified while only three images are misclassified.

5. Conclusion

The proposed a scalable deep mastering framework that permits building extra reusable and efficient deep fashions whilst a couple of correlated assets are to be had. in the case of volumetric multimodal MRI for Genius tumor segmentation, we proposed several scalable CNNs that combine smoothly the complementary records about tumor tissues scattered throughout the special image modalities. Scale Nets impose a sparse shape to the backend of the architecture wherein cross features and go modalities changes are separated. It is worth noticing that Scale Nets are related to the lately proposed implicit Conditional Networks and Deep-Rooted Networks that use in moderation connected architecture but do now not advocate the transposition of branches and grouped functions. each of those frameworks have been proven to improve the computational efficiency of contemporary CNNs by lowering the range of parameters, the amount of computation and growing the parallelization of the convolutions. the use of our proposed scalable layer structure, we readily adapted a compact network for brain percolation of monomial T1 right into a multimodal network for intelligence tumor segmentation with four distinct photograph modalities as enter. Scalable systems, way to their sparsity, have a regularization impact. Contrast of traditional and scalable CNNs indicates that scalable networks are extra robust and use fewer parameters at the same time as maintaining similar or higher accuracy for clinical picture segmentation. Scalable network systems have the ability to make deep network for clinical images more reusable. We accept as true with that scalable networks will play a key enabling function for efficient switch mastering in volumetric MRI analysis.

References

Tiwari, Arti, Shilpa Srivastava, and Millie Pant. "Brain tumor segmentation and classification from magnetic resonance images: Review of selected methods from 2014 to 2019." *Pattern Recognition Letters* 131 (2020): 244-260.

Bahadure, Nilesh Bhaskarrao, Arun Kumar Ray, and Har Pal Thethi. "Comparative approach of MRI-based brain tumor segmentation and classification using genetic algorithm." *Journal of digital imaging* 31 (2018): 477-489.

Biratu, Erena Siyoum, et al. "A survey of brain tumor segmentation and classification algorithms." *Journal of Imaging* 7.9 (2021): 179.

Sharif, Muhammad, et al. "Brain tumor segmentation and classification by improved binomial thresholding and multi-features selection." *Journal of ambient intelligence and humanized computing* (2018): 1-20.

Kumari, Nitu, and Sanjay Saxena. "Review of brain tumor segmentation and classification." *2018 International conference on current trends towards converging technologies (ICCTCT)*. IEEE, 2018.

JS Jufin and D Jeba Derwin. Normalized graph-cut based necrotic image segmentation of brain tumours. International Journal of Computer Science and Mobile Computing (IJCSMC), Volume2, (4), 2013

Jianhua Yao. Image processing in tumor imaging. New techniques in oncologic imaging, pages 79–102, 2006

Jung Leng Foo. A survey of user interaction and automation in medical image seg-mentation methods. Iowa State University, Human Computer Interaction Technical Report ISU-HCI-2006-02, 2006.

Andac Hamachi, Nadir Kucuk, Kutlay Karaman, Kayihan Engin, and Gozde Unal. Tumor-cut: segmentation of brain tumors on contrast enhanced MR images for radio-surgery applications. Medical Imaging, IEEE Transactions on, 31(3):790–804, 2012.

Tammy Riklin Raviv, KV Leemput, and Bjoern H Menze. Multi-modal brain tumor segmentation via latent atlases. Proceeding MICCAIBRATS, pages 64–73, 2012.

Xiaotao Guo, Lawrence Schwartz, and Binsheng Zhao. Semi-automatic segmentation of multimodal brain tumor using active contours. Multimodal Brain Tumor Segmentation, page 27, 2013.

Liang Zhao, Wei Wu, and Jason J Corso. Semi-automatic brain tumor segmentation by constrained mrfs using structural trajectories. In Medical Image Computing and Computer-Assisted Intervention–MICCAI 2013, pages 567–575. Springer, 2013.

Andac Hamamci, Nadir Kucuk, Kutlay Karaman, Kayihan Engin, and Gozde Unal. Tumor-cut: segmentation of brain tumors on contrast enhanced MR images for radio-surgery applications. Medical Imaging, IEEE Transactions on, 31(3):790–804, 2012.

EG Hoeffner, SK Mukherji, A Srinivasan, and DJ Quint. Neuroradiology back to the future: brain imaging. American Journal of Neuroradiology, 33(1):5–11, 2012.

Paul Jaccard. The distribution of the flora in the alpine zone. 1. New phytologist, 11(2):37–50, 1912.

Gregor Urban Ullrich Kothe Martin Bendszus Jens Kleesiek, Armin Biller and Fred Hamprecht. ilastik for multi-modal brain tumor segmentation. Multimodal Brain Tumor Segmentation, page 6, 2014.

JS Jufin and D Jeba Derwin. Normalized graph-cut based necrotic image segmentation of brain tumours. International Journal of Computer Science and Mobile Computing (IJCSMC), Volume2, (4), 2013.

Raphael Meier, Stefan Bauer, Johannes Slotboom, Roland Wiest, and Mauricio Reyes. A hybrid model for multimodal brain tumor segmentation. Multimodal Brain Tumor Segmentation, page 31, 2013.

Josiah Bloecher Bram Stieltjes Hans-Peter Meinzer Michael Goetz, Christian Weber and Klaus Maier-Hein. Extremely randomized trees based brain tumor segmentation. Multimodal Brain Tumor Segmentation, page 6, 2014.

Gayatri Mirajkar and Balaji Barbadekar. Automatic segmentation of brain tumors from MR images using undecimated wavelet transform and gabor wavelets. In Electronics, Circuits, and Systems (ICECS), 2010 17th IEEE International Conference on, pages 702–705. IEEE, 2010.

Fabian Pedregosa, Gaël Varoquaux, Alexandre Gramfort, Vincent Michel, Bertrand Thirion, Olivier Grisel, Mathieu Blondel, Peter Prettenhofer, Ron Weiss, Vincent Dubourg, et al. Scikit-learn: Machine learning in python. The Journal of Machine Learning Research, 12:2825–2830, 2011.

Karteek Popuri, Dana Cobzas, Martin Jagersand, Sirish L Shah, and Albert Murtha. 3d variational brain tumor segmentation on a clustered feature set. In SPIE Medical Imaging, pages 72591N–72591N. International Society for Optics and Photonics, 2009.

Tammy Riklin Raviv, KV Leemput, and Bjoern H Menze. Multi-modal brain tumor segmentation via latent atlases. Proceeding MICCAIBRATS, pages 64–73, 2012.

S Reza and KM Iftekharuddin. Multi-class abnormal brain tissue segmentation using texture. Multimodal Brain Tumor Segmentation, page 38, 2013.

M Schmidt. Automatic brain tumor segmentation. Master's thesis, University of Alberta, 2005.

Nick Tustison, Max Wintermark, Chris Durst, and Brian Avants. Ants and arboles. Multimodal Brain Tumor Segmentation, page 47, 2013.